Published in final edited form as:
Ann Neurol. 2020 December 01; 88(6): 1194–1204. doi:10.1002/ana.25911.

Neuroinflammation and tau co-localize *in vivo* in progressive supranuclear palsy

Maura Malpetti, MSc[1], **Luca Passamonti, PhD**[1,2], **Timothy Rittman, PhD**[1], **P. Simon Jones, MSc**[1], **Patricia Vázquez Rodríguez, PhD**[1], **W. Richard Bevan-Jones, PhD**[3], **Young T. Hong, PhD**[1,4], **Tim D. Fryer, PhD**[1,4], **Franklin I. Aigbirhio, PhD**[1], **John T. O'Brien, DM**[3,5,*], **James B. Rowe, PhD**[1,5,*]

[1]Department of Clinical Neurosciences, University of Cambridge, Cambridge, UK

[2]Institute of Molecular Bioimaging and Physiology, National Research Council, Milano, Italy

[3]Department of Psychiatry, University of Cambridge, Cambridge, UK

[4]Wolfson Brain Imaging Centre, University of Cambridge, Cambridge, UK

[5]Cambridge University Hospitals NHS Trust, Cambridge, UK

Abstract

Objective—We examined the relationship between tau pathology and neuroinflammation using [^{11}C]PK11195 and [^{18}F]AV-1451 PET in seventeen patients with progressive supranuclear palsy Richardson's syndrome (PSP). We tested the hypothesis that neuroinflammation and tau protein aggregation co-localize macroscopically, and correlate with clinical severity.

Methods—Non-displaceable binding potential (BP_{ND}) for each ligand was quantified in 83 regions of interest (ROIs). The [^{11}C]PK11195 and [^{18}F]AV-1451 BP_{ND} values were correlated across all regions. The spatial distributions of [^{11}C]PK11195 and [^{18}F]AV-1451 binding were determined by principal component analyses (PCAs), and the loading of each spatial component compared against the patients' clinical severity (using the PSP-rating-scale).

Results—Regional [^{11}C]PK11195 and [^{18}F]AV-1451 binding were positively correlated ($R=0.577$, $p<0.0001$). The PCA identified four components for each ligand, reflecting the relative expression of tau pathology or neuroinflammation in distinct groups of brain regions. Positive associations between [^{11}C]PK11195 and [^{18}F]AV-1451 components' loadings were found in both sub-cortical ($R=0.769$, $p<0.0001$) and cortical regions ($R=0.836$, $p<0.0001$). There were positive

Corresponding Author: Prof. James B. Rowe, Department of Clinical Neurosciences, University of Cambridge, Herchel Smith Building, Forvie Site, Robinson Way, Cambridge Biomedical Campus, Cambridge CB2 0SZ, Tel. no: +44 1223 760 696, james.rowe@mrc-cbu.cam.ac.uk.
*Joint senior authors

The authors have no conflicts of interest.

Author contributions
MM, JTO and JBR contributed to the conception and design of the study; MM, LP, TR, PSJ, PVR, WRBJ, YTH, TDF and FIA contributed to the acquisition and analysis of data; MM, LP, JTO and JBR contributed to drafting the text and preparing the figures.

Potential conflicts of interest
The authors have nothing to report.

correlations between clinical severity and both sub-cortical tau pathology (R=0.667, p=0.003) and neuroinflammation (R=0.788, p<0.001).

Interpretation—We show that tau pathology and neuroinflammation co-localize in PSP, and that individual differences in subcortical tau pathology and neuroinflammation are linked to clinical severity. Although longitudinal studies are needed to determine causal associations between these molecular pathologies, we suggest that the combination of tau- and immune-oriented strategies may be useful for effective disease-modifying treatments in PSP.

Introduction

Progressive supranuclear palsy (PSP) is a devastating neurodegenerative disorder caused by the neuro-glial aggregation of tau protein, particularly in the basal ganglia, diencephalon, and brainstem[1,2]. The classical clinical phenotype of PSP is Richardson's syndrome, with vertical supranuclear gaze palsy, akinetic-rigidity, falls, and cognitive decline[3,4]. The aggregation of misfolded and hyper-phosphorylated 4-repeats tau, in oligomers and successively into fibrillary tangles, is central to PSP pathology[1,2]. However, neuroinflammation also occurs in PSP, with microglial activation[5,6], with a proposed toxic alliance between tau-mediated neurodegeneration and neuroinflammation. In the related condition of frontotemporal dementia, tau burden and microglial activation are macroscopically co-localized[7].

Previous positron emission tomography (PET) has indicated changes in PSP using ligands targeting tau[8–16] and microglial activation[17,18]. However, previous work has not addressed whether *in vivo* tau pathology and microglial activation are related in PSP. Answering this question would shed new lights in the pathophysiological mechanisms underlying PSP and may facilitate the development of therapeutic strategies that synergistically target neuroinflammation and tau pathology in PSP.

We used [^{11}C]PK11195 PET to measure of microglial activation and [^{18}F]AV-1451 PET as an index of tau burden (see discussion regarding limitations of these ligands and their mitigation[19,20]). The latter binds to aggregated tau in Alzheimer's disease (AD) and, with lower affinity, to non-AD tauopathies[21]. It also does not distinguish tau- from TDP43-patholologies. However, this lack of specificity does not undermine its utility to test our hypotheses because: 1) the clinical-pathological correlation in PSP-Richardson's syndrome is very high[22]; 2) significant TDP43 pathology is exceedingly rare in PSP, and 3) [^{18}F]AV-1451 displays a specific anatomical pattern of binding that clearly distinguishes PSP from AD[8]. Moreover, to test our hypothesis, it is the distribution not relative affinity of binding that is critical. [^{11}C]PK11195 is widely used as a marker of microglial activation in neurodegenerative diseases[23], including PSP[17,18]. It binds the translocator protein (TSPO) on mitochondrial membranes in activated microglia. Although its sensitivity may be affected by its relatively low signal-to-noise ratio and low brain penetration, [^{11}C]PK11195 is not significantly influenced by common genetic polymorphisms that affect second generation TSPO ligands.

We test the hypothesis that neuroinflammation and tau protein aggregation co-localize, and correlate with clinical severity in PSP. We assessed the topography of this relationship with

Europe PMC Funders Author Manuscripts

Europe PMC Funders Author Manuscripts

[^{11}C]PK11195 PET and [^{18}F]AV-1451 PET using: (a) a region of interest (ROI) approach to study correlations across the brain; and (b) a set of spatial patterns determined by principal component analysis (PCA).

Methods

Participants

As part of the Neuroimaging of Inflammation in Memory and Related Other Disorders (NIMROD) study[24], we recruited 17 patients with a clinical diagnosis of probable PSP according to Movement Disorder Society (MDS) 1996 criteria. All patients also met the later MDS-PSP 2017 criteria for PSP-Richardson's syndrome[4]. Patients underwent PET scanning with both [^{11}C]PK11195 and [^{18}F]AV-1451, to respectively assess tau pathology and neuroinflammation. To minimise radiation exposure in healthy people, two groups of control participants were enrolled: n=16 underwent [^{11}C]PK11195 PET and n=15 underwent [^{18}F]AV-1451 PET. At the first visit, demographic and cognitive measures (i.e., the revised Addenbrooke's Cognitive Examination - ACE-R) were collected in all participants. Disease severity of patients was measured at the baseline visit and at six monthly intervals, using the PSP rating scale (PSP-RS). Participants had mental capacity to take part in the study and provided written informed consent. The protocol was approved by the National Research Ethic Service East of England Cambridge Central Committee and the UK Administration of Radioactive Substances Advisory Committee.

PET and MRI data acquisition and pre-processing

Full details of the imaging protocol are published elsewhere[8,18]. In brief, patients underwent 3T MRI together with [^{11}C]PK11195 and [^{18}F]AV-1451 PET, using dynamic imaging for 75 and 90 minutes respectively. MRI used Siemens Magnetom Tim Trio and Verio scanners (Siemens Healthineers, Erlangen, Germany), while PET used a GE Advance and a GE Discovery 690 PET/CT (GE Healthcare, Waukesha, USA). The use of identical emission data acquisition protocols and image reconstruction algorithms on the two scanners meant that the differences were effectively limited to the attenuation correction method (rotating rod ^{68}Ge/^{68}Ga transmission scan vs. a low dose CT scan) and the axial spatial resolution (6.8 mm FWHM vs. 5.1 mm FWHM). Regarding the attenuation correction, the CT (Hounsfield unit) to 511 keV linear attenuation coefficient transformation used on GE PET/CT systems is that of Burger et al[25], which was determined from data acquired with a GE Discovery LS PET/CT, the PET part of which is identical to the GE Advance, thereby enhancing the correspondence between GE PET and PET/CT systems. With respect to differences in spatial resolution, the primary data given in the paper are for large regions of interest. This will limit the impact of any spatial resolution differences, which for brain imaging on the scanners used mainly occur in the axial dimension. Furthermore, patient motion, together with resolution losses in image processing steps, such as realignment of dynamic image series and co-registration to MR, will reduce these differences. The interval between [^{11}C]PK11195 and [^{18}F]AV-1451 PET scans had mean and standard deviation (SD) of 1.2 ± 1.7 months. Eleven patients underwent [^{11}C]PK11195 and [^{18}F]AV-1451 PET scans using a GE Discovery scanner, while 6 patients underwent were scanned using a GE

Europe PMC Funders Author Manuscripts

Advance scanner. These two groups did not differ in demographic or clinical characteristics ($p>0.05$).

For each subject, the aligned dynamic PET image series for each scan was rigidly co-registered to the T1-weighted MRI image. BP_{ND} was calculated in 83 cortical and subcortical ROIs using a modified version of the n30r83 Hammersmith atlas (www.brain-development.org), which includes brainstem parcellation and the cerebellar dentate nucleus. Prior to kinetic modelling, regional PET data were corrected for partial volume effects from cerebrospinal fluid by dividing by the mean regional grey-matter plus white-matter fraction determined from SPM segmentation. For [^{11}C]PK11195, supervised cluster analysis was used to determine the reference tissue time-activity curve and BP_{ND} values were calculated in each ROI using a simplified reference tissue model with vascular binding correction[26]. For [^{18}F]AV-1451, BP_{ND} values were quantified in each ROI using a basis function implementation of the simplified reference tissue model, with superior cerebellar cortex grey matter as the reference region. This cerebellar region was selected as reference region given post-mortem evidence showing minimal tau pathology in PSP[8]. The same data acquisition and analysis approach was applied for the two control groups. In control groups, 10 individuals were scanned using the GE Discovery scanner (N=3 with [^{11}C]PK11195 and N=7 [^{18}F]AV-1451), and 21 were scanned using the GE Advance (N=13 with [^{11}C]PK11195 and N=8 [^{18}F]AV-1451).

Statistical analyses

Age, years of education, ACE-R total and fluency scores were compared between patients and controls with independent-samples t-tests, while sex was compared with the Chi-square test. A linear mixed effects model was applied to the longitudinal PSP-RS scores using R 4.0.0 and lme4 package (R Core Team, 2012). Estimated intercept and slope scores were extracted for each patient and used to estimate an individual PSP-RS score at the time of each PET scan (Figure 1). Statistical analysis proceeded in four steps.

First, to test whether microglial activation and tau pathology co-localized across the whole brain, we estimated the Pearson correlation of corresponding [^{11}C]PK11195 and [^{18}F]AV-1451 BP_{ND} group-average values across all 83 ROIs. We also applied a linear mixed effects model that takes into account the variability between subjects in both intercept and slope of the relation between the two tracers' regional binding. We compared three models: (i) an initial model with only a random intercept term for patients, (ii) a model with also the fixed effect of regional [11C]PK11195 PET values (x variable) on regional [18F]AV-1451 PET (y variable), and (iii) a model with uncorrelated random intercept and random slope terms. The R function permlmer() was used to perform permutation tests on the terms of interest in each model comparison.

Second, the number of ROIs was reduced from 83 to 43, averaging left and right regional BP_{ND} values, as in previous studies[8,18]. This step reduces the degrees of freedom, increasing power, and is justified in PSP in which the motor syndrome is essentially symmetric. Differences between PSP and controls in the ROIs were tested for each ligand with independent t-tests and false discovery rate (Benjamini-Hochberg FDR) correction for multiple comparisons.

Europe PMC Funders Author Manuscripts

Third, in PSP patients, BP_{ND} values in the 43 bilateral ROIs were included in separate PCAs for [^{11}C]PK11195 and [^{18}F]AV-1451. This reduces the data dimensionality further, identifying a small set of components that best explain the data variance. The resulting component reveal anatomical patterns covary in terms of neuroinflammation or tau pathology. The orthogonal varimax rotation was applied on the single PCA, separately for each ligand. This rotation serves to maximise the dispersion of loadings within components and to facilitate their interpretability (i.e., anatomical patterns of neuroinflammation and tau pathology). We selected components with eigenvalues >1, up to a cumulative total of >80% of variance explained. PET components were visualised with BrainNet Viewer[27].

Finally, to test for co-localization of microglial activation and tau pathology in specific neuroanatomical patterns of ligand binding, we performed Pearson correlations between individual scores of each ligand-specific component extracted. Bonferroni's method was used to correct for multiple comparisons. We also report the analyses adjusted for age, education and sex, or for variability in the time interval between PET scans, included as covariates of no interest. For each ligand, we tested for significant associations between regionally specific inter-modality correlating PCA clusters (i.e., anatomical patterns of neuroinflammation and tau pathology) and disease severity. For severity, we imputed PSP-RS scores for the time of each scan, using multivariate imputation by chain equations (*mice* function in R software). Patient id number, months from baseline to each follow-up visit, and all available PSP-RS scores were included in the multiple imputation. From this, 100 sets of PSP-RS scores were imputed for each PET scan, with N=50 iterations to generate each estimated dataset. The average value per participant across all 100 ligand-specific estimated PSP-RS scores (Figure 1, blue and red dots), was retained for correlation analyses with imaging components. These correlation analyses were repeated using a single raw PSP-RS score as clinical severity index, identified as the closest clinical assessment to both PET scans.

Data availability

Anonymized data may be shared by request to the senior author from a qualified investigator for non-commercial use (data sharing may be subject to restrictions according to consent and data protection legislation).

Results

Demographics, clinical and cognitive variables are summarized in Table 1. There were no significant group differences in age (t(46)= -0.14, 95% CI= -4.29 to 3.74, p=0.892) or sex (X^2(1)=0.230, 95% CI= -0.20 to 0.34, p=0.632). Differences between PSP and control groups were found in the ACE-R total scores (t(18.5)= -4.53, 95% CI= -17.42 to -6.39, p<0.001), fluency ACE-R sub-scores (t(21.1)= -6.11, 95% CI= -6.79 to -3.34, p<0.001), and years of education (t(46)= -3.64, 95% CI= -4.09 to -1.18, p=0.001). Estimated PSP-RS scores at the time of PET are also included in Table 1.

Europe PMC Funders Author Manuscripts

Regional [^{11}C]PK11195 and [^{18}F]AV-1451 BP_{ND} in PSP

Regional group mean [^{11}C]PK11195 BP_{ND} correlated with the corresponding [^{18}F]AV-1451 BP_{ND} across the whole brain (R=0.577, p<0.0001) (Figure 2A). At the group level, patients with PSP had high [^{11}C]PK11195 BP_{ND} in the brainstem, cerebellum, thalamus, and occipital and cingulate cortex, with pons and medulla having the highest values (pons: 0.19 ± 0.08; medulla: 0.23 ± 0.13). High [^{18}F]AV-1451 BP_{ND} was found in the basal ganglia, midbrain and thalamus (Figure 2A), with the basal ganglia having the highest value (mean=0.33; SD =0.10). The model comparisons on linear mixed effects models identified as optimal model the one with a fixed term for the effect of [^{11}C]PK11195 on [^{18}F]AV-1451 regional, and uncorrelated intercept and slope terms ($\Delta\chi^2$ (1) = 21.28, p = 3.972e-06, perm-p= 0.001). In this model, the effect of [^{11}C]PK11195 on [^{18}F]AV-1451 regional values at group level (fixed effect) was significant (Estimate=0.685, SD=0.053, Std Beta=0.550, 95% CI: 0.47 to 0.63, p = 2.2e-16, perm-p= 0.001) (Figure 2B). From the graphs (Figure 2), the basal ganglia macro-region did not appear to display a significant correlation, thus we repeated an analogous linear mixed effects model on regional binding potential values in basal ganglia only. Comparing this model with the one without the fixed effect of [^{11}C]PK11195 PET, the model comparison indicated a significant effect of [^{11}C]PK11195 on [^{18}F]AV-1451 values in these regions (Estimate=0.426, SD=0.133, Std Beta=0.280, 95% CI: 0.11 to 0.46; $\Delta\chi^2$ (1) = 8.82, p = 0.003, perm-p= 0.007)

[^{11}C]PK11195 binding values were higher in PSP patients than in controls in the putamen (t(31)=4.08, 95% CI= 0.029 to 0.085, p<0.001 uncorrected, p=0.013 FDR correction), and pallidum (t(31)=3.72, 95% CI= 0.045 to 0.155, p<0.001 uncorrected, p=0.017 FDR correction). Likewise, [^{18}F]AV-1451 binding was significantly increased in PSP, than controls, in the putamen (t(30)=3.66, 95% CI= 0.061 to 0.216, p<0.001 uncorrected, p=0.008 FDR correction), pallidum (t(30)=5.69, 95% CI= 0.160 to 0.339, p<0.001 uncorrected, p=0.0001 FDR correction), thalamus (t(30)=3.74, 95% CI= 0.044 to 0.149, p<0.001 uncorrected, p=0.008 FDR correction), midbrain (t(30)=3.84, 95% CI= 0.059 to 0.195, p<0.001 uncorrected, p=0.008 FDR correction), and dentate nucleus (t(30)=3.87, 95% CI= 0.046 to 0.150, p<0.001 uncorrected, p=0.008 FDR correction), confirming our previous findings [8,18]. We report only those comparisons that survived FDR correction at p<0.05. We repeated the group comparisons applying multiple regression analyses with group as predictor of region-specific tracer binding and age, education and sex as covariates. Including covariates, [^{11}C]PK11195 binding values were higher in PSP patients than in controls in the putamen (t(31)=3.68, 95% CI= 0.024 to 0.085, p<0.001 uncorrected, p=0.022 FDR correction), and pallidum (t(31)=3.95, 95% CI= 0.056 to 0.178, p<0.001 uncorrected, p=0.021 FDR correction). [^{18}F]AV-1451 binding values were higher in PSP patients than controls in pallidum (t(31)=3.81, 95% CI= 0.103 to 0.343, p<0.001 uncorrected, p=0.032 FDR correction), but also in thalamus, midbrain and dentate cerebellum gyrus when considering uncorrected p-values <0.05. We do not further discuss this group comparison as the principal aim of this study was to study the co-localization of [^{11}C]PK11195 and [^{18}F]AV-1451 binding in PSP.

Europe PMC Funders Author Manuscripts

Principal component analysis of [^{11}C]PK11195 and [^{18}F]AV-1451 BP_{ND} in PSP

For [^{11}C]PK11195 BP_{ND}, four components were identified which collectively explained 81.4% of the data variance (Figure 3, left panel). Component 1 reflected [^{11}C]PK11195 binding in posterior cortical regions, the orbitofrontal cortex and cerebellar grey-matter (62.9% of the total variance). Component 2 grouped together medial and superior regions of the temporal lobe including the amygdala, hippocampus and para-hippocampal gyrus, as well as other cortical areas such as the insula and temporo-parietal junction (9.2% variance). Component 3 was weighted to brainstem regions (i.e., midbrain and pons), the dentate nucleus, and the cerebellar white-matter (5.1% variance). Component 4 comprised superior and medial frontal regions (4.3% variance).

Likewise, four components were found for [^{18}F]AV-1451 BP_{ND} which explained together 81.8% of the data variance (Figure 3, right panel). Component 1 reflected global [^{18}F]AV-1451 cortical binding, especially in frontal cortical regions (61.3% of the total variance). Component 2 reflected [^{18}F]AV-1451 BP_{ND} binding in the insula and medial temporal lobe regions (e.g. amygdala, hippocampus) (8.6% variance). Component 3 loaded onto the anterior superior temporal gyrus and frontal subgenual cortex (7.0% variance). Component 4 was weighted towards subcortical areas including the midbrain, pons, substantia nigra, thalamus, dentate nucleus and cerebellar white matter (5.0% variance).

Correlation between [^{11}C]PK11195 and [^{18}F]AV-1451 principal components in PSP

After adjusting for Bonferroni correction (p=0.05/16 correlations between [^{18}F]AV-1451 and [^{11}C]PK11195 components), Pearson correlations between individual loading scores for the four [^{11}C]PK11195 components and the four [^{18}F]AV-1451 components showed two significant results (Figure 4): 1) [^{11}C]PK11195 component #2 positively correlated with [^{18}F]AV-1451 component #2 (R=0.836, 95% CI= 0.594 to 0.939, p<0.001), and 2) [^{11}C]PK11195 component #3 positively correlated with [^{18}F]AV-1451 component #4 (R=0.769, 95% CI= 0.458 to 0.913, p<0.001). Importantly, these correlations remained significant after correcting for age, education and sex ([^{11}C]PK11195 #2 - [^{18}F]AV-1451 #2: R=0.781, 95% CI= 0.480 to 0.917, p<0.001; [^{11}C]PK11195 #3 - [^{18}F]AV-1451 #4: R=0.742, 95% CI= 0.406 to 0.901, p=0.002), or for the variability in the time interval between PET scans ([^{11}C]PK11195 #2 - [^{18}F]AV-1451 #2: R=0.804, 95% CI= 0.526 to 0.926, p<0.001; [^{11}C]PK11195 #3 - [^{18}F]AV-1451 #4: R=0.792, 95% CI= 0.503 to 0.922, p<0.001). The correlations also remained significant when PET scanner type (GE Advance/GE Discovery) was included as covariate ([^{11}C]PK11195 #2 - [^{18}F]AV-1451 #2: R=0.796, 95% CI= 0.510 to 0.923, p<0.001; [^{11}C]PK11195 #3 - [^{18}F]AV-1451 #4: R=0.776, 95% CI= 0.471 to 0.915, p<0.001).

The individual PCA-derived scores for ligand-specific subcortical components separately correlated with disease severity (PSP-RS) (Figure 5). The imputed PSP-RS scores for the time of PET correlated highly with the nearest actual PSP-RS assessment ([^{11}C]PK11195, R=0.948, 95% CI= 0.858 to 0.981, p<0.0001; and [^{18}F]AV-1451, R=0.965, 95% CI= 0.902 to 0.987, p<0.0001). Considering the imputed PSP-RS at the time of the PET scans, both [^{11}C]PK11195 component #3 (R=0.788, 95% CI= 0.496 to 0.920, p<0.001) and [^{18}F]AV-1451 component #4 (R=0.667, 95% CI= 0.275 to 0.869, p=0.003) positively

correlated with disease severity (Figure 5). These correlations remained significant after correcting for age, education and sex ([^{11}C]PK11195 #3: R=0.773, 95% CI= 0.464 to 0.914, p=0.001; [^{18}F]AV-1451 #4: R=0.671, 95% CI= 0.280 to 0.871, p=0.009). We then applied a linear model to test whether the interaction between [^{11}C]PK11195 component #3 and [^{18}F]AV-1451 component #4 predicts PSP-RS. The interaction term was not significant in the model with the estimated PSP-RS score, adjusted to the time midway between the PET scans (p=0.883). Similar results were obtained using the closest raw PSP-RS to the PET scans as clinical severity measure.

Discussion

This study suggests that microglial activation and tau protein aggregation are co-localized in PSP, macroscopically. The relationship between neuroinflammation and tau pathology is observed across widespread brain regions, although it is most evident in a subset of cortical regions (i.e. insula and temporo-parietal junction) and subcortical structures (i.e. brainstem and cerebellum). This co-localization resembles that observed between protein aggregation and microglial activation in both Tau- and TDP43-associated forms of frontotemporal lobar degeneration observed by *post mortem* immunohistochemistry and *in vivo* with the ligands used in this PET study[7]. The *in vivo* measures of neuroinflammation and tau burden in the brainstem and cerebellum were both associated with disease severity.

Before considering the implications of our findings for the pathogenesis of PSP, we discuss the caveats associated with the PET ligands. Although [^{18}F]AV-1451 shows strong *in vivo* and post-mortem binding to tau pathology in AD, it displays variable affinity in healthy aging and non-AD tauopathies[28–30]. The tracer also binds to non-tau proteinopathies (i.e., is positive in TDP43 pathology with C9orf72 mutations and semantic dementia[31]), and other targets such as neuromelanin[29], choroid plexus[28] and monoamine oxidase (MAO)[32]. However, 'off-target' binding can neither fully account for [^{18}F]AV-1451 signal in striatum or cortex – as previous *post mortem* analyses reveal that no neuromelanin accumulates there[8,33] – nor in choroid plexus as histological analysis revealed tangle-like inclusions in its epithelial cells[34]. The [^{18}F]AV-1451 'off-target' binding to MAO[32] expressed on reactive astrocytes and activated microglia[32,35], could in principle contribute to correlated binding of the two ligands. However, a previous report of a carrier of a MAPT genetic mutation described high [^{11}C]PK11195 binding in the absence of significant [^{18}F]AV-1451 binding[36], which suggests that despite the potential for a common target, the two ligands are not equivalent in their binding. Furthermore, affinity of [^{18}F]AV-1451 for monoamine oxidase is weak and the use of MAO-inhibitors does not significantly displace [^{18}F]AV-1451 binding in patients with tauopathies[37]. Nevertheless, we acknowledge that the affinity of [^{18}F]AV-1451 to the 4-repeat tau in non-AD tauopathies as PSP is lower than its affinity to 3/4-repeat AD-related tau pathology[29,30]. In PSP, higher [^{18}F]AV-1451 binding has been found in sub-cortical rather than cortical regions (the reverse for AD), consistent with the well-established cortical versus sub-cortical distribution of PSP-Richardson's syndrome[8–10,13,14,16]. This supports the use of [^{18}F]AV-1451 PET to quantify and localize tau pathology in different tauopathies with clear and known pathologic substrates, such as PSP.

The [^{11}C]PK11195 ligand is selective for activated microglia over quiescent microglia or reactive astrocytes[38], but, it has been criticised for its relatively low signal-to-noise ratio and low brain penetration which may affect its sensitivity to activated microglia. Nevertheless, this would reduce effect sizes and increase type II errors, rather than leading to false positive findings. Second-generation PET radioligands for TSPO are characterised by higher signal-noise ratio than [^{11}C]PK11195 but their binding is markedly affected by single nucleotide polymorphisms (rs6971) which cause heterogeneity in PET data and require genetic screening. [^{11}C]PK11195 binding is less affected by this polymorphism, and has well established methods of kinetic analysis[39]. Hence, [^{11}C]PK11195 PET was the ligand of choice for this study of PSP.

With these caveats in mind, we turn to our principal results. To study the *in vivo* co-localization between microglial activation and tau pathology in PSP, we applied correlation analyses between binding of the two ligands 1) across all brain regions, and 2) between principal components of a set of bilateral brain regions, extracted to reduce complexity of the imaging data. With the first approach, we found a positive correlation at group level between [^{11}C]PK11195 and [^{18}F]AV-1451 binding across the whole brain (Figure 2A), which remained significant also after accounting for the variability between patients (Figure 2B). This indicates a close association between microglial activation and tau pathology in PSP that extensively involves subcortical and cortical regions. This finding aligns with *in vivo* correlation between neuroinflammation and tau aggregation in AD and frontotemporal dementia[7,40]. Collectively, these multi-tracer PET studies support previous *in vitro* evidence of the association between microglial activation and tau aggregation in different tauopathies[41]. The spatial distribution of this *in vivo* association between microglial activation and tau pathology in PSP mirrors previous findings showing that tau pathology affects not only subcortical but also cortical regions in PSP Richardson's syndrome[42,43].

When assessing the ligand-specific components from principal component analysis, we found a positive correlation between [^{11}C]PK11195 and [^{18}F]AV-1451 binding in brainstem and cerebellar regions, loaded into anatomically overlapping components of both ligands (Figure 4, right panel). This association occurs in motor-related regions that are involved in the neuropathology and symptomatology of PSP (i.e. functional deficits, postural instability, and supranuclear gaze palsy) associated with PSP Richardson's syndrome[44]. Of note, both tau pathology and microglial activation in the brainstem-cerebellar component correlated with disease severity, using either the imputed PSP-RS scores for time of PET scans (Figure 5) or the score of the closest PSP-RS assessment to PET scans. This finding adds relevant information to the literature as only a few previous studies have explored how [^{11}C]PK11195 and [^{18}F]AV-1451 binding relate to disease severity in PSP[8,9,13,14,16,18]. In our sample, although the two components individually correlate with clinical severity, they did not interact in their association with PSP-RS. This suggests an additive and partially independent effect of the two pathological processes on clinical progression rather than a synergistic effect, although larger sample sizes and longitudinal designs will need to explore this relationship further.

[^{11}C]PK11195 and [^{18}F]AV-1451 binding were also correlated in a cortical component (Figure 4, left panel), which for both ligands was weighted towards regions of the medial

temporal lobe, insula and temporo-parietal junction. Previous studies have implicated the medial temporal lobe and limbic structures in basic emotional recognition, which is in turn found to be impaired in PSP, alongside theory of mind and social cognition[45,46]. While recognition of happiness was reported to be preserved in patients with PSP, their recognition of negative emotions (i.e. anger, disgust, surprise, fear and sadness) has been reported as affected[45]. Basal ganglia, insula and amygdala have been reported to be implicated in the recognition of predominately negative emotions, and these neuropsychological function is abnormal in PSP[43,46]. the association between microglial activation and tau pathology we found in limbic regions may complement biological explanations of emotion-related and social deficits in PSP. However, longitudinal studies are needed to clarify the timing of these interacting effects on pathological and clinical disease progression.

Our finding of tau and neuroinflammation co-localization in the cortex of patients with PSP Richardson's syndrome is in keeping with previous post-mortem evidence showing tau pathology and atrophy not only in subcortical and limbic regions, but also in the parietal lobe[43]. Specifically, the supramarginal gyrus has been described as the most affected brain region in two independent pathological cohorts of patients with PSP Richardson's syndrome[43]. The absence of *in vivo* evidence about supramarginal atrophy in the literature may enhance the importance of the demonstrated association between neuroinflammation and tau accumulation in this region as an early biomarker of later-stage neuronal loss.

Our study has limitations. First, we acknowledge the limited power of the analyses related to the relatively small size of our sample. Although our cohort is larger than many previous multi-tracer PET studies on rare neurodegenerative diseases like PSP, larger and independent replication samples would be helpful. Second, the recruitment was based on clinical diagnosis, which was confirmed at each follow-up visit; however, post-mortem pathological confirmation was available only in 8 patients. However, all 8 had PSP, and over 95% of patients with a clinical diagnosis of PSP-Richardson's syndrome have PSP pathology or related 4R-tuaopathy. Third, our results are based on a cross-sectional design, which cannot be used to infer causal relationship between tau and microglial activation. A longitudinal assessment of tau burden, microglial activation and clinical progression alongside mediation analyses are necessary next steps to clarify the interplay between the two pathological processes and their effect on disease severity across time.

To conclude, our results confirm the relevance of neuroinflammation to PSP-Richardson's syndrome and a close association with tau pathology. Our findings indicate a macroscopic anatomical relationship between neuroinflammation and tau pathology. Although we cannot infer the causal direction in the relationship between pathological mechanisms, we speculate that microglial activation may be activated by an initial tau misfolding and contribute to tau pathology and propagation. The latter, in turn, may lead to further neuroinflammation, as previously suggested in AD (see review[41]). Pre-clinical research suggests that microglial activation may precede the formation of tangles[47] and then promote the spreading of pathological tau[48]. Our findings suggest that the co-localization of neuroinflammation and tau pathology is an important pathogenetic mechanism in PSP, and both processes may be involved in defining PSP clinical severity. A better understanding of the interaction between the pathological substrates in PSP and its effects on disease progression may crucially

contribute to improving patients' stratification and clinical trials. Specifically, our results encourage the application of [^{11}C]PK11195 and [^{18}F]AV-1451 PET as markers of co-localized pathological mechanisms in PSP to develop new targeting therapies and empower clinical trials.

Acknowledgments

This study was co-funded by the National Institute for Health Research (NIHR) Biomedical Research Centre (Grant Reference Number 146281); the PSP Association ("MAPT-PSP"); the Wellcome Trust (JBR 103838); the Cambridge Trust & Sidney Sussex College Scholarship; the Medical Research Council (MR/P01271X/1); and the Cambridge Centre for Parkinson-Plus. The views expressed are those of the authors and not necessarily those of the NIHR or the Department of Health and Social Care. We thank our participant volunteers for their participation in this study, and the radiographers/technologists at the Wolfson Brain Imaging Centre and Addenbrooke's PET/CT Unit, and the research nurses of the Cambridge Centre for Parkinson-plus for their invaluable support in data acquisition. We thank the East Anglia Dementias and Neurodegenerative Diseases Research Network (DeNDRoN) for help with subject recruitment, and Drs Istvan Boros, Joong-Hyun Chun, and other WBIC RPU staff for the manufacture of the radioligands. We thank Avid (Lilly) for supplying the precursor for the production of [^{18}F]AV-1451 used in this study. We also thank Dr. Thomas Cope and Dr. Kamen Tsvetanov for discussion.

References

1. Dickson DW, Rademakers R, Hutton ML. Progressive supranuclear palsy: Pathology and genetics. Brain Pathol. 2007; 17:74–82. [PubMed: 17493041]
2. Kovacs, GG, Lukic, MJ, Irwin, DJ. , et al. Distribution patterns of tau pathology in progressive supranuclear palsyActa Neuropathol [online serial]. Vol. 140. Springer; Berlin Heidelberg: 2020. 99–119.
3. Williams DR, De Silva R, Paviour DC, et al. Characteristics of two distinct clinical phenotypes in pathologically proven progressive supranuclear palsy: Richardson's syndrome and PSP-parkinsonism. Brain. 2005; 128:1247–1258. [PubMed: 15788542]
4. Höglinger GU, Respondek G, Stamelou M, et al. Clinical diagnosis of progressive supranuclear palsy: The movement disorder society criteria. Mov Disord. 2017; 32:853–864. [PubMed: 28467028]
5. Ishizawa K, Dickson DW. Microglial activation parallels system degeneration in progressive supranuclear palsy and corticobasal degeneration. J Neuropathol Exp Neurol. 2001; 60:647–657. [PubMed: 11398841]
6. Fernández-Botrán R, Ahmed Z, Crespo FA, et al. Cytokine expression and microglial activation in progressive supranuclear palsy. Parkinsonism Relat Disord. 2011; 17:683–688. [PubMed: 21741294]
7. Bevan-Jones WR, Cope TE, Jones PS, et al. Neuroinflammation and protein aggregation co-localize across the frontotemporal dementia spectrum. Brain. 2020; 143:1010–1026. [PubMed: 32179883]
8. Passamonti L, Vázquez Rodríguez P, Hong YT, et al. ^{18}F-AV-1451 positron emission tomography in Alzheimer's disease and progressive supranuclear palsy. Brain.
9. Cho H, Choi JY, Hwang MS, et al. Subcortical ^{18}F-AV-1451 binding patterns in progressive supranuclear palsy. Mov Disord. 2017; 32:134–140. [PubMed: 27813160]
10. Hammes J, Bischof GN, Giehl K, et al. Elevated in vivo [18F]-AV-1451 uptake in a patient with progressive supranuclear palsy. Mov Disord. 2017; 32:170–171. [PubMed: 27476874]
11. Kepe V, Bordelon Y, Boxer A, et al. PET imaging of neuropathology in tauopathies: progressive supranuclear palsy. J Alzheimers Dis. 2013; 36:145–153. [PubMed: 23579330]
12. Ishiki, a; Harada, R; Okamura, N; , et al. Tau imaging with [18F]THK-5351 in progressive supranuclear palsy. Eur J Neurol. 2017; 24:130–136. [PubMed: 27797445]
13. Smith R, Schain M, Nilsson C, et al. Increased basal ganglia binding of 18F-AV-1451 in patients with progressive supranuclear palsy. Mov Disord. 2017; 32:108–114. [PubMed: 27709757]
14. Whitwell JL, Lowe VJ, Tosakulwong N, et al. [18F]AV-1451 tau positron emission tomography in progressive supranuclear palsy. Mov Disord. 2017; 32:124–133. [PubMed: 27787958]

15. Brendel M, Schönecker S, Höglinger G, et al. [18F]-THK5351 PET Correlates with Topology and Symptom Severity in Progressive Supranuclear Palsy. Front Aging Neurosci. 2018; 9:1–12.
16. Schonhaut DR, McMillan CT, Spina S, et al. 18F-flortaucipir tau positron emission tomography distinguishes established progressive supranuclear palsy from controls and Parkinson disease: A multicenter study. Ann Neurol. 2017; 82:622–634. [PubMed: 28980714]
17. Gerhard A, Trender-Gerhard I, Turkheimer F, Quinn NP, Bhatia KP, Brooks DJ. In vivo imaging of microglial activation with [11C](R)-PK11195 PET in progressive supranuclear palsy. Mov Disord. 2006; 21:89–93. [PubMed: 16108021]
18. Passamonti L, Rodríguez PV, Hong YT, et al. [11C]PK11195 binding in Alzheimer disease and progressive supranuclear palsy. Neurology [online serial]. 2018; 90:e1989–e1996. DOI: 10.1212/WNL.0000000000005610
19. Boche D, Gerhard A, Rodriguez-Vieitez E. Prospects and challenges of imaging neuroinflammation beyond TSPO in Alzheimer's disease. Eur J Nucl Med Mol Imaging [online serial]. European Journal of Nuclear Medicine and Molecular Imaging. 2019; 46:2831–2847. DOI: 10.1007/s00259-019-04462-w
20. Leuzy A, Chiotis K, Lemoine L, et al. Tau PET imaging in neurodegenerative tauopathies—still a challenge. Mol Psychiatry.
21. Hall, B, Mak, E, Cervenka, S, Aigbirhio, FI, Rowe, JB, O'Brien, JT. Ageing Res Rev [online serial]. Vol. 36. Elsevier B.V; 2017. In vivo tau PET imaging in dementia: Pathophysiology, radiotracer quantification, and a systematic review of clinical findings; 50–63.
22. Gazzina S, Respondek G, Compta Y, et al. Neuropathological validation of the MDS-PSP criteria with PSP and other frontotemporal lobar degeneration. bioRxiv [online serial].
23. Stefaniak J, O'Brien J. Imaging of neuroinflammation in dementia: a review. J Neurol Neurosurg Psychiatry [online serial]. 2015; 87doi: 10.1136/jnnp-2015-311336
24. Bevan-Jones WR, Surendranathan A, Passamonti L, et al. Neuroimaging of Inflammation in Memory and Related Other Disorders (NIMROD) study protocol: a deep phenotyping cohort study of the role of brain inflammation in dementia, depression and other neurological illnesses. BMJ Open [online serial]. 2017; 7:e013187.doi: 10.1136/bmjopen-2016-013187
25. Burger C, Goerres G, Schoenes S, Buck A, Lonn A, Von Schulthess G. PET attenuation coefficients from CT images: Experimental evaluation of the transformation of CT into PET 511-keV attenuation coefficients. Eur J Nucl Med. 2002; 29:922–927.
26. Yaqub M, Van Berckel BNM, Schuitemaker A, et al. Optimization of supervised cluster analysis for extracting reference tissue input curves in (R)-[11C]PK11195 brain PET studies. J Cereb Blood Flow Metab. 2012; 32:1600–1608. [PubMed: 22588187]
27. Xia M, Wang J, He Y. BrainNet Viewer: a network visualization tool for human brain connectomics. PLoS One. 2013; 8:e68910. [PubMed: 23861951]
28. Lowe VJ, Curran G, Fang P, et al. An autoradiographic evaluation of AV-1451 Tau PET in dementia. Acta Neuropathol Commun [online serial] Acta Neuropathologica Communications. 2016; 4:1–19. DOI: 10.1186/s40478-016-0315-6 [PubMed: 26727948]
29. Marquié M, Normandin MD, Vanderburg CR, et al. Validating novel tau positron emission tomography tracer [F-18]-AV-1451 (T807) on postmortem brain tissue. Ann Neurol [online serial]. 2015; 78:787–800.
30. Sander K, Lashley T, Gami P, et al. Characterization of tau positron emission tomography tracer [18F]AV-1451 binding to postmortem tissue in Alzheimer's disease, primary tauopathies, and other dementias. Alzheimer's Dement. 2016; 12:1116–1124. [PubMed: 26892233]
31. Bevan-Jones WR, Cope TE, Jones PS, et al. [18F]AV-1451 binding in vivo mirrors the expected distribution of TDP-43 pathology in the semantic variant of primary progressive aphasia. J Neurol Neurosurg Psychiatry [online serial]. 2018; 89:1032–1037. DOI: 10.1136/jnnp-2017-316402
32. Vermeiren C, Motte P, Viot D, et al. The tau positron-emission tomography tracer AV-1451 binds with similar affinities to tau fibrils and monoamine oxidases. Mov Disord. 2018; 33:273–281. [PubMed: 29278274]
33. Hansen AK, Knudsen K, Lillethorup TP, et al. In vivo imaging of neuromelanin in Parkinson's disease using 18F-AV-1451 PET. Brain. 2016; 139:2039–2049. [PubMed: 27190023]

34. Ikonomovic MD, Abrahamson EE, Price JC, Mathis CA, Klunk WE. [F-18]AV-1451 positron emission tomography retention in choroid plexus: More than “off-target” binding. Ann Neurol. 2016; 80:307–308. [PubMed: 27314820]
35. Saura J, Luque JM, Cesura AM, et al. Increased monoamine oxidase B activity in plaque-associated astrocytes of Alzheimer brains revealed by quantitative enzyme radioautography. Neuroscience [online serial]. 1994; 62:15–30.
36. Bevan-Jones WR, Cope TE, Jones PS, et al. In vivo evidence for pre-symptomatic neuroinflammation in a MAPT mutation carrier. Ann Clin Transl Neurol. 2019; 6:373–378. [PubMed: 30847369]
37. Hansen AK, Brooks DJ, Borghammer P. MAO-B Inhibitors Do Not Block In Vivo Flortaucipir([18F]-AV-1451) Binding. Mol Imaging Biol Molecular Imaging and Biology. 2018; 20:356–360. [PubMed: 29127552]
38. Banati RB. Visualising microglial activation in vivo. Glia. 2002; 40:206–217. [PubMed: 12379908]
39. Turkheimer FE, Edison P, Pavese N, et al. Reference and target region modeling of [11C]-(R)-PK11195 brain studies. J Nucl Med. 2007; 48:158–167. [PubMed: 17204713]
40. Dani M, Wood M, Mizoguchi R, et al. Microglial activation correlates in vivo with both tau and amyloid in Alzheimer’ s disease. :1–15.
41. Vogels T, Murgoci AN, Hromádka T. Intersection of pathological tau and microglia at the synapse. Acta Neuropathol Commun. 2019; 7:109. [PubMed: 31277708]
42. Dickson DW, Ahmed Z, Algom AA, Tsuboi Y, Josephs KA. Neuropathology of variants of progressive supranuclear palsy. Curr Opin Neurol. 2010; 23:394–400. [PubMed: 20610990]
43. Schofield EC, Hodges JR, Macdonald V, Cordato NJ, Kril JJ, Halliday GM. Cortical atrophy differentiates Richardson’s syndrome from the parkinsonian form of progressive supranuclear palsy. Mov Disord. 2011; 26:256–263. [PubMed: 21412832]
44. Williams, DR, Lees, AJ. Lancet Neurol [online serial]. Vol. 8. Elsevier Ltd; 2009. Progressive supranuclear palsy: clinicopathological concepts and diagnostic challenges; 270–279.
45. Ghosh BCP, Rowe JB, Calder AJ, Hodges JR, Bak TH. Emotion recognition in progressive supranuclear palsy. J Neurol Neurosurg Psychiatry. 2009; 80:1143–1145. [PubMed: 19762901]
46. Ghosh BCP, Calder AJ, Peers PV, et al. Social cognitive deficits and their neural correlates in progressive supranuclear palsy. Brain. 2012; 135:2089–2102. [PubMed: 22637582]
47. Yoshiyama Y, Higuchi M, Zhang B, et al. Synapse Loss and Microglial Activation Precede Tangles in a P301S Tauopathy Mouse Model. Neuron. 2007; 53:337–351. [PubMed: 17270732]
48. Asai H, Ikezu S, Tsunoda S, et al. Depletion of microglia and inhibition of exosome synthesis halt tau propagation. Nat Neurosci. 2015; 18:1584–1593. [PubMed: 26436904]

Europe PMC Funders Author Manuscripts

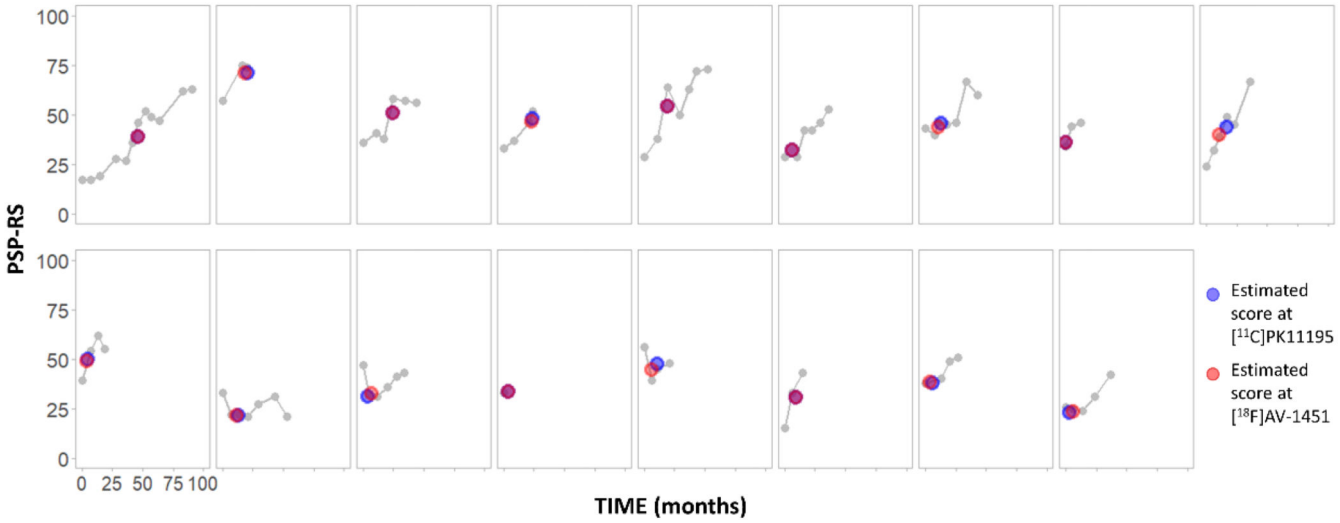

Figure 1.

Longitudinal PSP-RS scores for each patient (grey), and estimated PSP-RS scores at the time of [11C]PK11195 PET (blue) and [18F]AV-1451 PET (red).

Europe PMC Funders Author Manuscripts

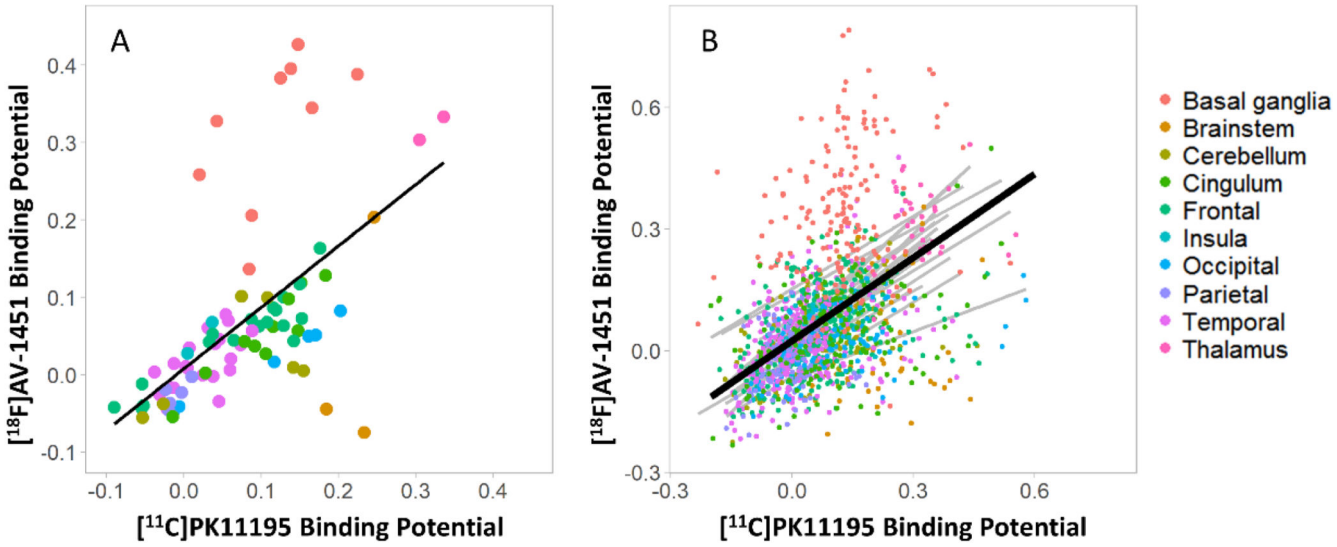

Figure 2.

Whole brain correlation between regional mean non-displaceable binding potential (BP_{ND}) of [^{11}C]PK11195 and [^{18}F]AV-1451 in the PSP group. Panels A: each point represents the average value across all patients for a specific brain region, while. Panel B: dots represent individual regional values for each patient, the black line represents the association between the two tracers at group level, while grey lines are individual correlations, within each patient. In both panels, colours indicate brain macro-areas reported on the right.

Europe PMC Funders Author Manuscripts

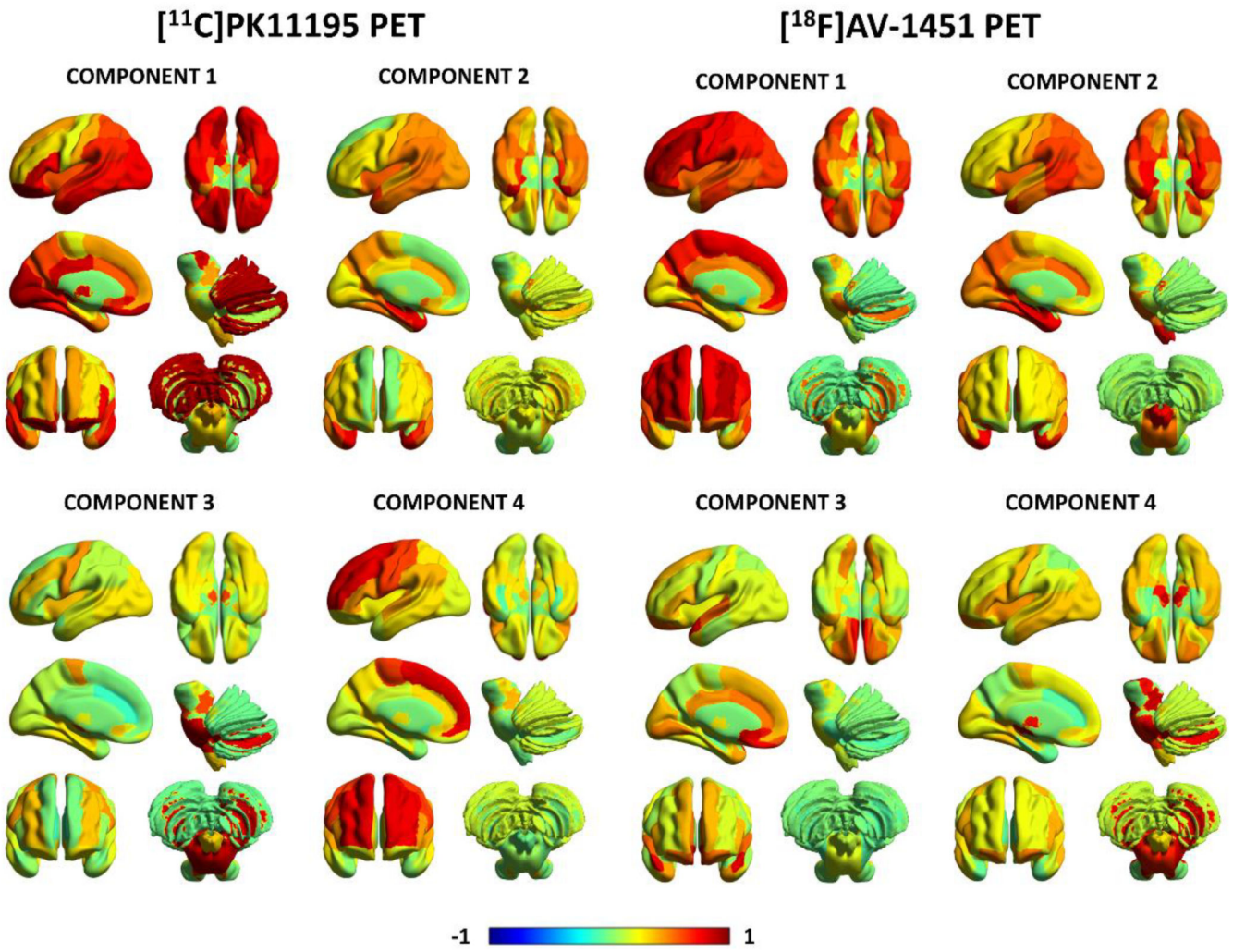

Figure 3.

First four principal components for [^{11}C]PK11195 non-displaceable binding potential (BP_{ND}) and [^{18}F]AV-1451 BP_{ND} in PSP. The colours represent the rotated weights of all brain regions for each component.

Europe PMC Funders Author Manuscripts

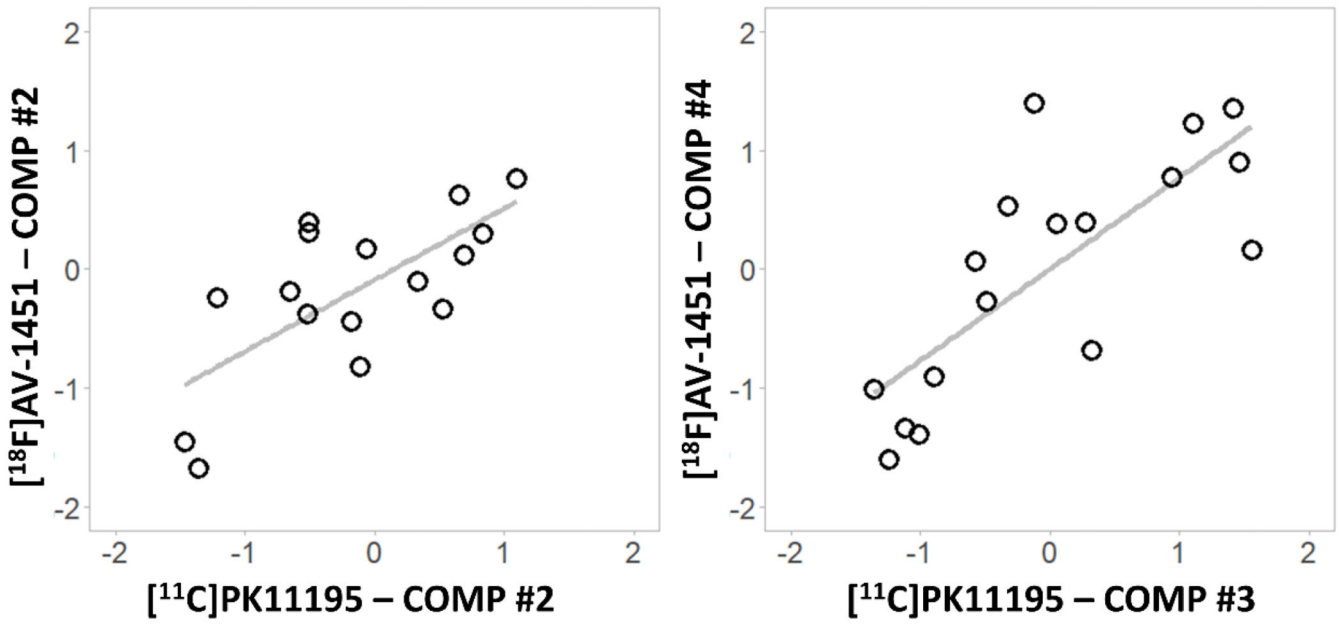

Figure 4.
Significant correlations between [^{11}C]PK11195 and [^{18}F]AV-1451 individual principal component (comp) scores.

Europe PMC Funders Author Manuscripts

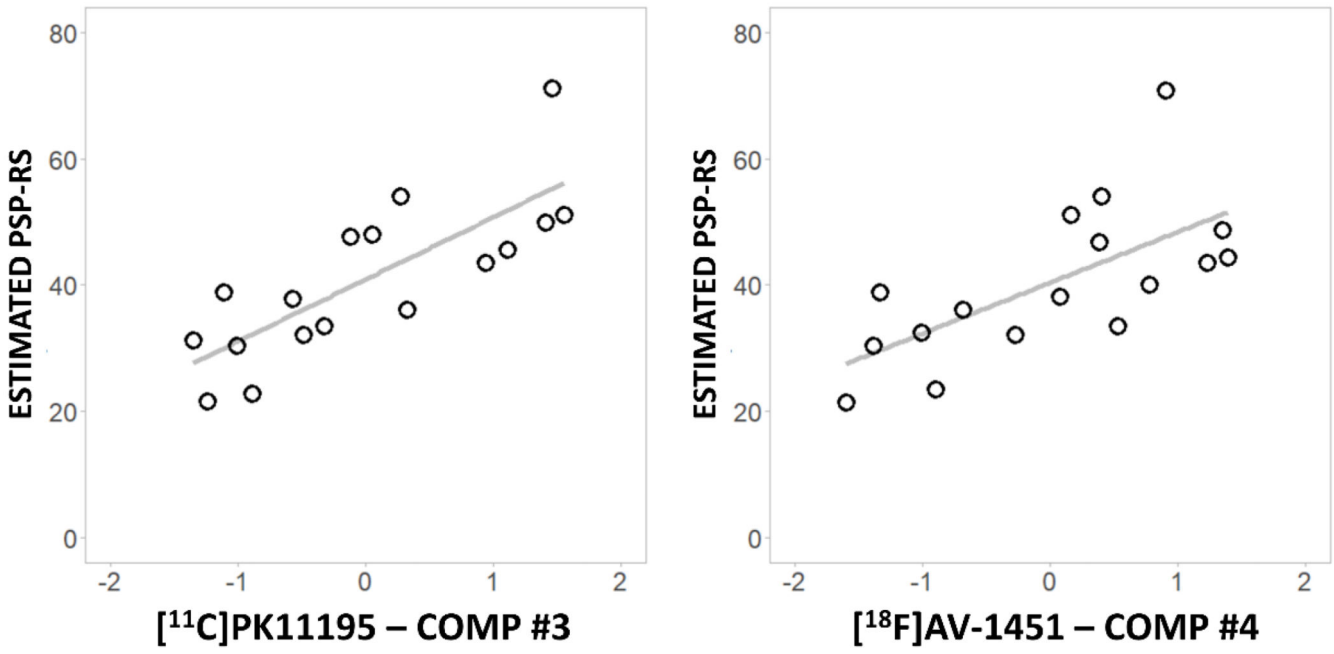

Figure 5.

Significant correlations between subcortical [^{11}C]PK11195 (left) and [^{18}F]AV-1451 (right) component (comp) scores and estimated PSP-RS at the time of each PET scan.